

## Estimating ground-level PM<sub>2.5</sub> using aerosol optical depth determined from satellite remote sensing

Aaron van Donkelaar,<sup>1</sup> Randall V. Martin,<sup>1,2</sup> and Rokjin J. Park<sup>3</sup>

Received 15 December 2005; revised 9 May 2006; accepted 25 July 2006; published 2 November 2006.

[1] We assess the relationship of ground-level fine particulate matter (PM<sub>2.5</sub>) concentrations for 2000–2001 measured as part of the Canadian National Air Pollution Surveillance (NAPS) network and the U.S. Air Quality System (AQS), versus remote-sensed PM<sub>2.5</sub> determined from aerosol optical depths (AOD) measured by the Moderate Resolution Imaging Spectroradiometer (MODIS) and the Multiangle Imaging Spectroradiometer (MISR) satellite instruments. A global chemical transport model (GEOS-CHEM) is used to simulate the factors affecting the relation between AOD and PM<sub>2.5</sub>. AERONET AOD is used to evaluate the method ( $r = 0.71$ ,  $N = 48$ , slope = 0.69). We find significant spatial variation of the annual mean ground-based measurements with PM<sub>2.5</sub> determined from MODIS ( $r = 0.69$ ,  $N = 199$ , slope = 0.82) and MISR ( $r = 0.58$ ,  $N = 199$ , slope = 0.57). Excluding California significantly increases the respective slopes and correlations. The relative vertical profile of aerosol extinction is the most important factor affecting the spatial relationship between satellite and surface measurements of PM<sub>2.5</sub>; neglecting this parameter would reduce the spatial correlation to 0.36. In contrast, temporal variation in AOD is the most influential parameter affecting the temporal relationship between satellite and surface measurements of PM<sub>2.5</sub>; neglecting daily variation in this parameter would decrease the correlation in eastern North America from 0.5–0.8 to less than 0.2. Other simulated aerosol properties, such as effective radius and extinction efficiency have a minor role temporally, but do influence the spatial correlation. Global mapping of PM<sub>2.5</sub> from both MODIS and MISR reveals annual mean concentrations of 40–50  $\mu\text{g}/\text{m}^3$  over northern India and China.

**Citation:** van Donkelaar, A., R. V. Martin, and R. J. Park (2006), Estimating ground-level PM<sub>2.5</sub> using aerosol optical depth determined from satellite remote sensing, *J. Geophys. Res.*, *111*, D21201, doi:10.1029/2005JD006996.

### 1. Introduction

[2] Exposure to fine particulate matter with diameter less than 2.5  $\mu\text{m}$  (PM<sub>2.5</sub>) has numerous negative effects upon human health, including cancers of the lung, pulmonary inflammation and cardiopulmonary mortality [Atkinson *et al.*, 2001; Pope *et al.*, 2002]. Global measurements of these aerosols would be valuable to epidemiological studies, the design of air quality control strategies, and air quality forecasting [Al-Saadi *et al.*, 2005].

[3] The launch of the Moderate Resolution Imaging Spectroradiometer (MODIS) and the Multiangle Imaging Spectroradiometer (MISR) instruments onboard NASA's Terra satellite in 1999 has provided global measurements of aerosol optical depth (AOD), a measure of light extinc-

tion by aerosol in the atmospheric column, during their overpass time of 1030 local time (LT). The temporal correlation between space-based measurements of AOD and surface PM concentrations has received considerable attention [i.e., Engel-Cox *et al.*, 2004a, 2004b, 2005; Chu *et al.*, 2003]. The quality of the correlation varies greatly with region, generally being much higher over the eastern United States as compared to the western United States [Al-Saadi *et al.*, 2005]. Empirical relationships between remotely measured AOD and surface PM<sub>2.5</sub> have been developed for the southeast United States using both MODIS [Wang and Christopher, 2003] and MISR [Liu *et al.*, 2005]. A common concern is the dependence upon several factors in addition to the AOD measurement, including the aerosol vertical profile, aerosol type and atmospheric conditions. Liu *et al.* [2004a] developed a simple, yet effective approach to correct for spatial and seasonal variation in these factors by applying local scaling factors from a global atmospheric chemistry model to AOD retrieved from MISR:

$$\text{Estimated PM}_{2.5} = \frac{\text{Model surface aerosol concentration}}{\text{Model AOD}} \times \text{Retrieved AOD} \quad (1)$$

<sup>1</sup>Department of Physics and Atmospheric Science, Dalhousie University, Halifax, Nova Scotia, Canada.

<sup>2</sup>Also at Harvard-Smithsonian Center for Astrophysics, Cambridge, Massachusetts, USA.

<sup>3</sup>Division of Engineering and Applied Sciences and Department of Earth and Planetary Sciences, Harvard University, Cambridge, Massachusetts, USA.

Here we investigate the relationship between satellite-measured AOD and surface PM<sub>2.5</sub> at satellite overpass time. Section 2 presents an explicit formulation of the factors involved and our approach to determine surface PM<sub>2.5</sub>. In section 3 we compare ground-level PM<sub>2.5</sub> against concentrations estimated from both MODIS and MISR AOD. We also validate this approach using AERONET AOD to estimate PM<sub>2.5</sub>. We then assess temporal and spatial variability of the parameters in that relationship to determine which factors deserve the most attention to improve PM<sub>2.5</sub> estimates derived from satellite measurements of AOD. Finally, we provide conclusions regarding the most influential parameters on the accuracy of this technique.

## 2. Determination of PM<sub>2.5</sub> From Satellite Measurements of AOD

[4] We first develop an explicit formulation of the relationship between AOD and PM<sub>2.5</sub> in order to isolate the parameters involved. Then we describe our simulation of that relationship.

### 2.1. AOD-PM Relation

[5] AOD,  $\tau$ , and total column aerosol mass loading  $\Omega$  are related by:

$$\Omega = \frac{4}{3} \frac{\rho r_{eff} \tau}{Q_e} \quad (2)$$

where  $\rho$  is the aerosol mass density at ambient relative humidity,  $r_{eff}$  is the column averaged effective radius (defined as the ratio of the third to second moment of an aerosol size distribution at ambient relative humidity), and  $Q_e$  is the column averaged extinction efficiency.

[6] Similarly, by accounting for the relative vertical profile of aerosol extinction, the aerosol mass concentration  $M_{\Delta z}$  between the ground and altitude  $\Delta z$  can be expressed as

$$M_{\Delta z} = \left[ \frac{4}{3} \frac{\rho_{\Delta z} r_{\Delta z, eff} f_{\Delta z}}{Q_{\Delta z, e}} \right] \tau \quad (3)$$

where  $f$  represents the fractional optical thickness below altitude  $\Delta z$ . All parameters in the bracketed expression refer to representative values below altitude  $\Delta z$ .

[7] Surface PM<sub>2.5</sub> measurements are usually of dry aerosol mass as described in section 3. Assuming spherical aerosols and accounting for aerosol hygroscopicity, the dry mass of PM<sub>2.5</sub> at the surface can be expressed as:

$$M_{2.5, d, \Delta z} = \left[ \frac{4}{3} \left( \frac{r_{2.5, d, \Delta z, eff}}{r_{2.5, \Delta z, eff}} \right)^3 \left( \frac{\rho_{2.5, d, \Delta z} r_{2.5, \Delta z, eff} f_{2.5, \Delta z}}{Q_{2.5, e, \Delta z}} \right) \right] \tau \quad (4)$$

where the subscript  $d$  indicates dry conditions and the subscript 2.5 denotes aerosols smaller than 2.5  $\mu\text{m}$  in diameter.  $M_{2.5, d, \Delta z}$  is the total fine dry aerosol mass between the surface and altitude  $\Delta z$ ,  $r_{2.5, d, \Delta z, eff}$  is the fine dry effective radius, and  $f_{2.5, \Delta z}$  is the ratio of fine AOD below altitude  $\Delta z$  to the total AOD. This equation assumes uniform aerosol properties between the surface and altitude

$\Delta z$ . We refer to  $M_{2.5, d, \Delta z}$  as remote-sensed PM<sub>2.5</sub>. Equation (4) reduces to equation (1) if a model is used to provide the values within the brackets.

### 2.2. Simulation of Parameters Affecting AOD-PM Relation

[8] We use a chemical transport model (GEOS-CHEM) to calculate the values within brackets in equation (4). The GEOS-CHEM chemical transport model (<http://www-as.harvard.edu/chemistry/trop/geos/index.html>) is driven by assimilated meteorological data from the Goddard Earth Observing System (GEOS-3) at the NASA Global Modeling Assimilation Office (GMAO). Meteorological fields include surface properties, humidity, temperature, winds, cloud properties, heat flux and precipitation. We use GEOS-CHEM v7-02-01 with 30 levels and 50 tracers using a  $1^\circ \times 1^\circ$  nested model version for North America and the adjacent oceans (10–60°N, 40–140°W) with dynamic boundary conditions from a global  $4^\circ \times 5^\circ$  simulation. A detailed description of this one-way nesting in the GEOS-CHEM model is given by Wang *et al.* [2004]. The lowest five levels are centered at approximately 10, 50, 100, 200 and 300 meters; a typical value for  $\Delta z$ , the lowest model level in equation (4), is approximately 20 m, varying with surface pressure. We assume that PM<sub>2.5</sub> concentration does not vary substantially from the surface to this height.

[9] The GEOS-CHEM aerosol simulation includes the sulfate-nitrate-ammonium system, carbonaceous aerosols, mineral dust, and sea salt. The aerosol and oxidant simulations are coupled through formation of sulfate and nitrate [Park *et al.*, 2004], heterogeneous chemistry [Jacob, 2000] and aerosol effects of photolysis rates [Martin *et al.*, 2003]. Wet and dry deposition are based upon Liu *et al.* [2001], including both washout and rainout of hydrophilic carbonaceous species. Primary organic aerosol emissions are assumed to be 50% hydrophilic, while secondary organic aerosols are assumed to have a wet scavenging efficiency of 80% [Park *et al.*, 2003]. We use seasonal average biomass burning inventories based upon climatological emissions. Anthropogenic carbon emission estimates are based upon Cooke *et al.* [1999] over North America, with imposed seasonal variation from Park *et al.* [2003]. Secondary organic chemistry is based upon the work by Chung and Seinfeld [2002]. The dust simulation is from T. D. Fairlie *et al.* (The impact of transpacific transport of mineral dust in the United States, submitted to *Atmospheric Environment*, 2006).

[10] Previous evaluations of the aerosol simulation have found a high degree of consistency with observations. Annual mean simulated sulfate concentrations explain 75–90% of the spatial variance in surface measurements from the IMPROVE network with little bias; slight underestimates are found versus IMPROVE for organic and elemental carbon ( $r^2 = 0.67$ , slope = 0.74;  $r^2 = 0.84$ , slope = 0.85, respectively) [Park *et al.*, 2004]. The simulated vertical variation in aerosol extinction is typically within 25% of lidar observations at the DOE/ARM site in Oklahoma and Cheju Island in South Korea [Hu *et al.*, 2006].

[11] We conduct a near 2 year simulation over January 2001 to October 2002. The GEOS-3 meteorological fields used for our simulation are not available after October 2002.

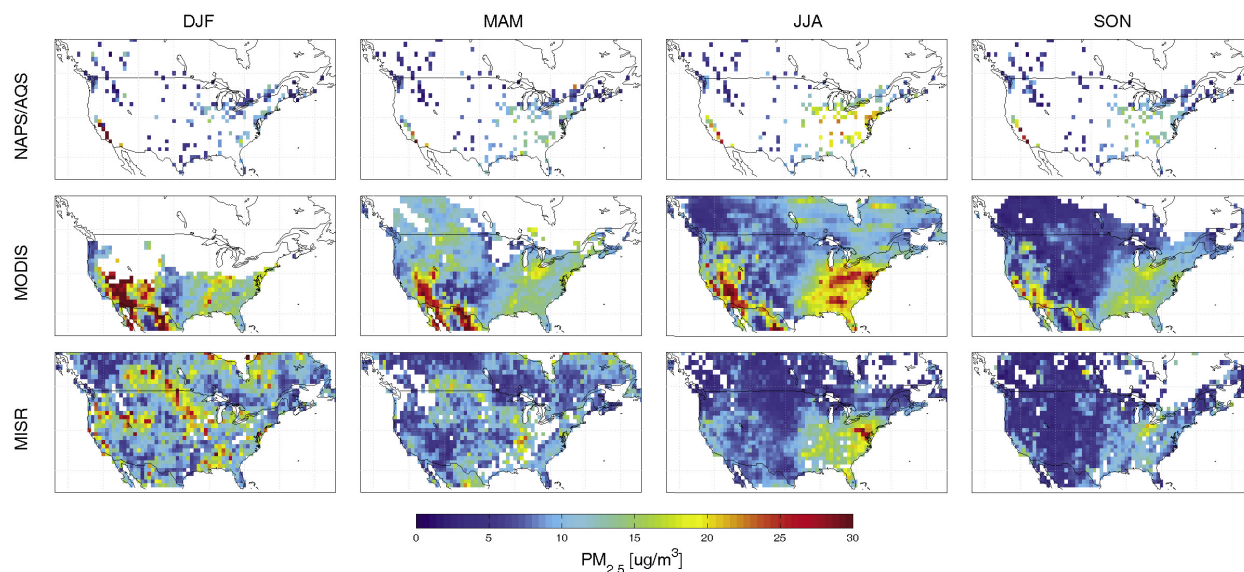


**Figure 1.** Seasonal average of surface PM<sub>2.5</sub> concentrations for December–February (DJF), March–May (MAM), June–August (JJA), September–November (SON) during the period from January 2001 to October 2002. (top) Ground-level measurements from the combined NAPS/AQS network. (middle and bottom) Determined respectively from MODIS and MISR measurements of aerosol optical depth (AOD). AOD measurements above 1.5 were discarded to reduce cloud contamination. White areas indicate ocean or regions with AOD measurements on fewer than either 40% of days for MODIS or 8% of days for MISR.

Local values for each parameter in equation (4) are taken from the simulation for each day at the MODIS and MISR overpass times between 1000 and 1200 local time. The parameters in equation (4) for each aerosol type are treated individually as an external mixture.

### 3. Measurements of Surface PM<sub>2.5</sub>

[12] Here we compare ground-based measurements of surface PM<sub>2.5</sub> with remote-sensed concentrations determined from AOD using the relationship in section 2.

#### 3.1. Ground-Based Surface PM<sub>2.5</sub>

[13] The ground-based measurements are from Environment Canada’s National Air Pollution Surveillance (NAPS) Network and the U.S. Environmental Protection Agency’s Air Quality System (AQS). Both networks collect continuous measurements primarily from tapered element oscillating microbalance (TEOM) instruments, which infer the collected PM<sub>2.5</sub> mass from changes in the natural frequency of the oscillator. Samples are heated to 30°–50°C to ensure dry conditions.

[14] Figure 1 (top) shows seasonal mean PM<sub>2.5</sub> concentrations taken on the hour, between 1000 and 1200 LT inclusive, as measured by the combined NAPS/AQS network from January 2001 to October 2002. PM<sub>2.5</sub> in the northeast United States exhibits a seasonal maximum during summer, corresponding to higher sulfate levels produced by increased SO<sub>2</sub> oxidation rates [Chin *et al.*, 2000]. Elevated PM<sub>2.5</sub> in California is associated with high emissions of aerosol precursors and topography that is exacerbated in winter by low mixing height, coupled with the thermody-

namic tendency for ammonium nitrate to exist in aerosol phase at lower wintertime temperatures [Blanchard and Tanenbaum, 2003]. Southeastern PM<sub>2.5</sub> concentrations are driven largely by organics, emitted directly by fires and formed as secondary organic aerosol from biogenic hydrocarbons; processes which are most active during warm seasons [Malm *et al.*, 2004].

#### 3.2. Surface PM<sub>2.5</sub> Estimated From MODIS AOD

[15] The MODIS aerosol retrieval is summarized by Remer *et al.* [2005]. Seven channels are used: 0.47, 0.55, 0.66, 0.87, 1.24, 1.64 and 2.1  $\mu\text{m}$ . MODIS provides near global coverage on a daily basis. Radiation exiting the atmosphere can be approximated as a function of optical depth, scattering phase function and single-scattering albedo when over a dark surface [Kaufman *et al.*, 1997]. Over land, the MODIS aerosol algorithm exploits this relation to measure optical depth by locating dark surfaces with the 2.1  $\mu\text{m}$  channel that is transparent to fine-mode particles and by empirically relating the 2.1  $\mu\text{m}$  measurements to surface properties at visible wavelengths. A simple model provides additional information on single scattering albedo and scattering phase function, with look-up tables used to determine aerosol properties at 0.47 and 0.66  $\mu\text{m}$ . Over water, spatial variability in the 0.55  $\mu\text{m}$  channel, high reflectance in the 0.47  $\mu\text{m}$  channel and infrared channels are all used to locate and avoid pixels contaminated with clouds. The 1.38  $\mu\text{m}$  channel is used to locate cirrus clouds. Chu *et al.* [2003] found significant agreement between MODIS and AERONET measurements of AOD ( $r = 0.82\text{--}0.91$ , slope = 0.83). MODIS retrievals of AOD over desert and coastal sites are, however, biased high because of errors caused by surface

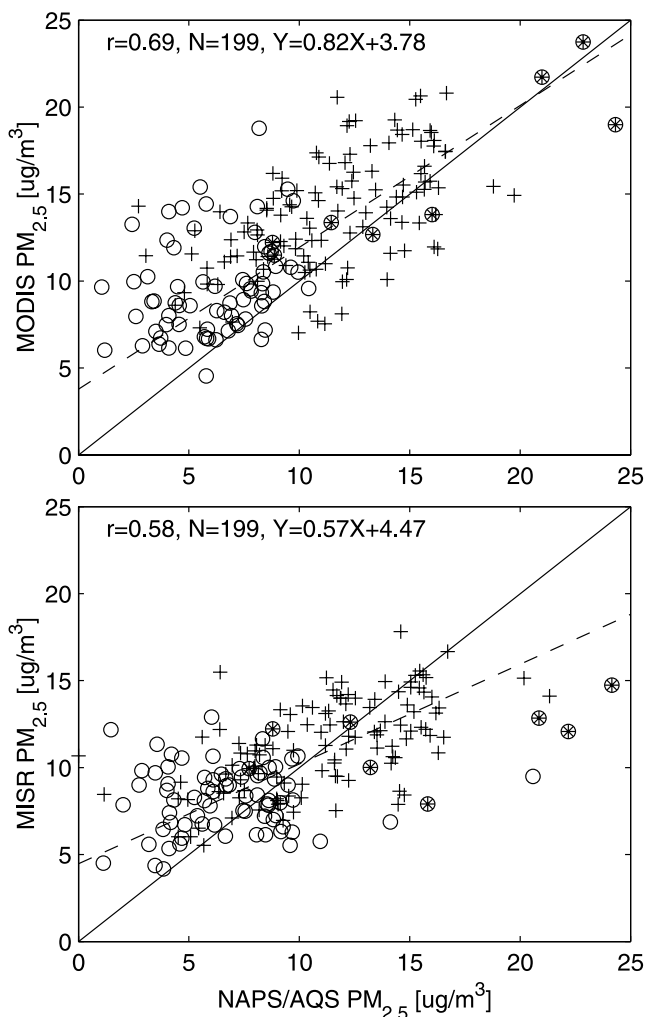


**Figure 2.** Comparison of average surface PM<sub>2.5</sub> from January 2001 to October 2002 determined from ground measurements versus surface PM<sub>2.5</sub> inferred from MODIS and MISR measurements of aerosol optical depth. NAPS/AQS averages are compiled between 1000 and 1200 LT, during successful overpass measurements. Eastern (crosses) and western (circles) sites are separated at 96°W. Measurements of the California region are indicated by circled stars. The solid line represents  $y = x$ . The dashed line was calculated with reduced major axis linear regression [Hirsch and Gilroy, 1984].

brightness and subpixel water contamination [Abdou *et al.*, 2005].

[16] Figure 1 (middle) shows seasonally averaged PM<sub>2.5</sub> concentrations calculated using 1° × 1°, daily level-3 version 4 MODIS AOD in equation (4). MODIS-estimated PM<sub>2.5</sub> generally compares well with the surface measurements, capturing both a similar structure and magnitude. Both show a seasonal maximum over the eastern United States during summer and low values in the Midwest throughout the year. However, surprisingly high values of surface PM<sub>2.5</sub> are found in the southwestern United States where few PM<sub>2.5</sub> measurements exist from AQS. Measurements from the Interagency Monitoring of Protected Visual Environments (IMPROVE) network indicate much lower

PM<sub>2.5</sub> concentrations in this region than we observe with MODIS [Malm *et al.*, 2004], suggesting an artifact in the retrieval. PM<sub>2.5</sub> determined from MODIS typically overpredicts surface measurements by 3–5 ug/m<sup>3</sup> at coastal sites on the Atlantic ocean and the Gulf of Mexico.

[17] Figure 2 (top) compares annual averages of coincident daily MODIS PM<sub>2.5</sub> and surface PM<sub>2.5</sub> for January 2001 to October 2002. A significant correlation ( $r = 0.69$ ) with a slope of 0.82 is found between MODIS PM<sub>2.5</sub> and surface PM<sub>2.5</sub>. However, MODIS PM<sub>2.5</sub> is biased high by 5.1 ug/m<sup>3</sup> on average.

### 3.3. Surface PM<sub>2.5</sub> Estimated From MISR AOD

[18] The MISR retrieval algorithm is summarized by Martonchik *et al.* [2002]. MISR is fitted with nine cameras having aft and forward viewing angles of 70.5°, 60.0°, 45.6°, 26.1° and nadir viewing at four spectral bands of 0.446, 0.558, 0.672 and 0.866 um. The MISR instrument requires between 6 and 9 days for complete global coverage because of its smaller across track viewing angle compared to MODIS. The MISR algorithm infers the surface-leaving and path radiance contributions to total observed radiance without any assumption regarding the absolute surface reflectance by observing radiometric changes leaving the top of the atmosphere from a single location but at different viewing angles. The surface-leaving radiance is then compared against precalculated values contained in look-up tables to determine the best fitting aerosol composition and associated AOD. MISR AOD and AERONET are generally consistent, with correlation coefficients ranging from ~0.7 to 0.9 depending upon region [Kahn *et al.*, 2005; Liu *et al.*, 2004b].

[19] Figure 1 (bottom) shows remote-sensed PM<sub>2.5</sub> calculated using daily level-3 MISR AOD in equation (4). Locations having less than 8% of days during the period of study represented were removed. This threshold is necessarily lower than MODIS owing to MISR's 6–9 day global coverage. MISR PM<sub>2.5</sub> is generally consistent with surface measurements during summer, however, more scatter is evident in winter. MISR PM<sub>2.5</sub> concentrations in the southwest are only 10–20% of MODIS PM<sub>2.5</sub> concentrations, and more consistent with GEOS-CHEM simulations. Concentrations in California remain biased low versus NAPS/AQS measurements. Accurate measurements of AOD are expected over bright surfaces such as deserts [Martonchik *et al.*, 2004]. The bias may result from a regional bias in GEOS-CHEM ammonium nitrate [Park *et al.*, 2006]. An underestimate of surface emissions in GEOS-CHEM would influence the vertical structure in equation (4), lowering remote-measured PM<sub>2.5</sub> concentrations.

[20] Figure 2 (bottom) compares MISR PM<sub>2.5</sub> against NAPS/AQS measurements. The correlation between MISR PM<sub>2.5</sub> and NAPS/AQS PM<sub>2.5</sub> is significant ( $r = 0.58$ ,  $N = 199$ ), with a slope of 0.57 and a mean positive bias of 3.1 ug/m<sup>3</sup>. The correlation and slope found here for MISR are lower than that given by Liu *et al.* [2004a] where California was excluded from the comparison. The removal of California from comparison improves the comparison with MISR PM<sub>2.5</sub> ( $r = 0.61$ ,  $N = 189$ , slope = 0.68) with little effect versus MODIS PM<sub>2.5</sub> ( $r = 0.67$ ,  $N = 189$ , slope = 0.93). Another major difference between these two studies is the spatial resolution of the analysis. Maintaining the removal of California while degrading the

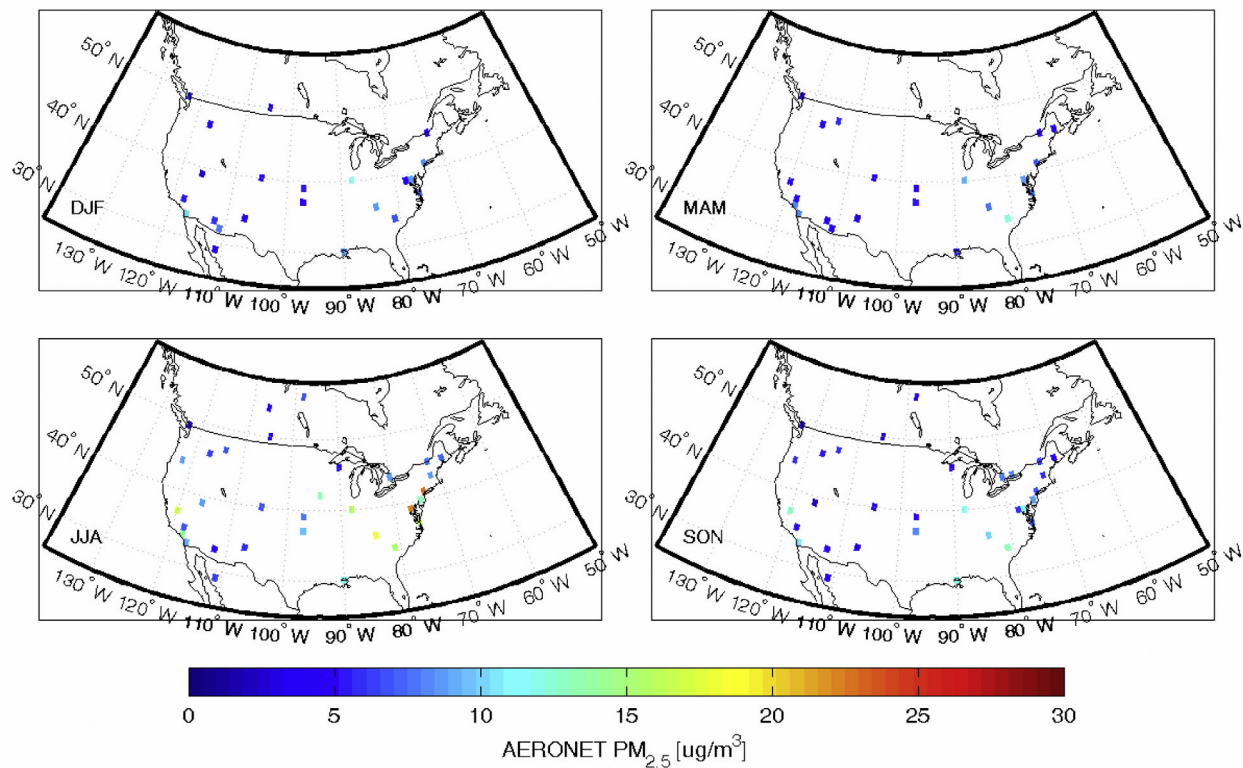


**Figure 3.** Seasonally averaged AERONET-derived PM<sub>2.5</sub> concentrations January 2001 to October 2002. AOD were taken between 1000 and 1200 LT and required to have measurements on at least 8% of days per season.

resolution of MISR PM<sub>2.5</sub> to 2° by 2° further improves the correlation ( $r = 0.69$ , slope = 0.70) with surface measurements. Similarly degrading MODIS PM<sub>2.5</sub> results in little change ( $r = 0.69$ , slope = 0.86). Model developments from GEOS-CHEM v5-07-08 used by Liu *et al.* [2004a] to v7-01-02 used here also contributes to differences in the relationship between MISR PM<sub>2.5</sub> and surface values.

### 3.4. Surface PM<sub>2.5</sub> Estimated From AERONET AOD

[21] The Aerosol Robotic Network (AERONET) is a globally distributed network of CIMEL spectral radiometers operating at seven spectral bands (0.34, 0.38, 0.44, 0.50, 0.67, 0.87 and 1.02  $\mu\text{m}$ ). A detailed description of these automatic-tracking, sun and diffuse sky radiometers is given by Holben *et al.* [1998]. AERONET measurements of AOD have an uncertainty of  $\sim 0.01$ – $0.02$  [Holben *et al.*, 2001]. Determination of surface PM<sub>2.5</sub> from AERONET could provide a test of our method by reducing uncertainties associated with satellite-based AOD measurements.

[22] Figure 3 shows PM<sub>2.5</sub> determined from level 2.0 AERONET AOD using equation (4). We find a significant seasonal and spatial relationship with ground-based PM<sub>2.5</sub> ( $r = 0.71$ ,  $N = 48$ , slope = 0.69), biased low by an average of 2.5  $\mu\text{g}/\text{m}^3$ . If California is excluded from the statistics the relationship improves to  $r = 0.80$ ,  $N = 43$ , slope = 0.89. AERONET PM<sub>2.5</sub> shows low concentrations throughout the southwest, in contrast with MODIS PM<sub>2.5</sub>, providing evidence of a regional bias in MODIS AOD, since other parameters from equation (4) have remained constant regardless of AOD source. This is consistent with Abdou

*et al.* [2005], who found that MODIS AOD is biased against AERONET in desert regions.

[23] PM<sub>2.5</sub> determined from AERONET AOD in California is substantially underpredicted, as was found for MISR PM<sub>2.5</sub>. This regional bias may reflect a weak gradient in the model extinction profile, as noted earlier. As a result, the apparent superior performance of MODIS PM<sub>2.5</sub> over MISR PM<sub>2.5</sub> in California may result from a positive bias in MODIS AOD combined with an unrealistic vertical structure that underestimates the fraction of AOD near the surface.

## 4. Factors Affecting the Relationship Between Retrieved and Measured Surface PM<sub>2.5</sub>

[24] An advantage of using equation (4) for PM<sub>2.5</sub> prediction is that it allows the isolation of individual variables and thereby the assessment of which parameters must be represented most accurately. Here we investigate each variable for both spatial and temporal variation over the time period of this study.

[25] Table 1 summarizes the most important factors affecting the spatial correlation of mean surface and remotely measured PM<sub>2.5</sub> as determined by replacing each parameter with a representative constant. Spatial variation in the relative vertical profile of modeled aerosol extinction has the largest effect on the accuracy of both mean remote PM<sub>2.5</sub> measurements; neglect of this parameter in MODIS and MISR reduces the spatial correlation versus surface measurements to 0.36 and 0.37, respectively. The AOD itself also exhibits significant influence on the accuracy of

**Table 1.** Spatial Correlation Coefficient,  $r$ , Between Remote PM<sub>2.5</sub> and Surface Measurements

	MODIS	MISR
Standard	0.69	0.58
Constant vertical structure ( $f_{2.5,\Delta z}$ )	0.36	0.37
Constant AOD	0.58	0.46
Constant aerosol properties ( $Q_{2.5,e}$ , $\tau_{2.5,\Delta z,eff}$ ; $\tau_{2.5,d,\Delta z,eff}$ ; $\rho_{2.5,d,\Delta z}$ )	0.61	0.40

remotely measured surface concentrations with respect to surface measurements. The spatial distribution of other aerosol properties is of little importance, except in the California region, which drives a significant change in the correlation when aerosol properties are held constant.

[26] Figure 4 shows the temporal relationship between remote and surface measurements of PM<sub>2.5</sub> under the same conditions as Table 1. Strong temporal correlation with

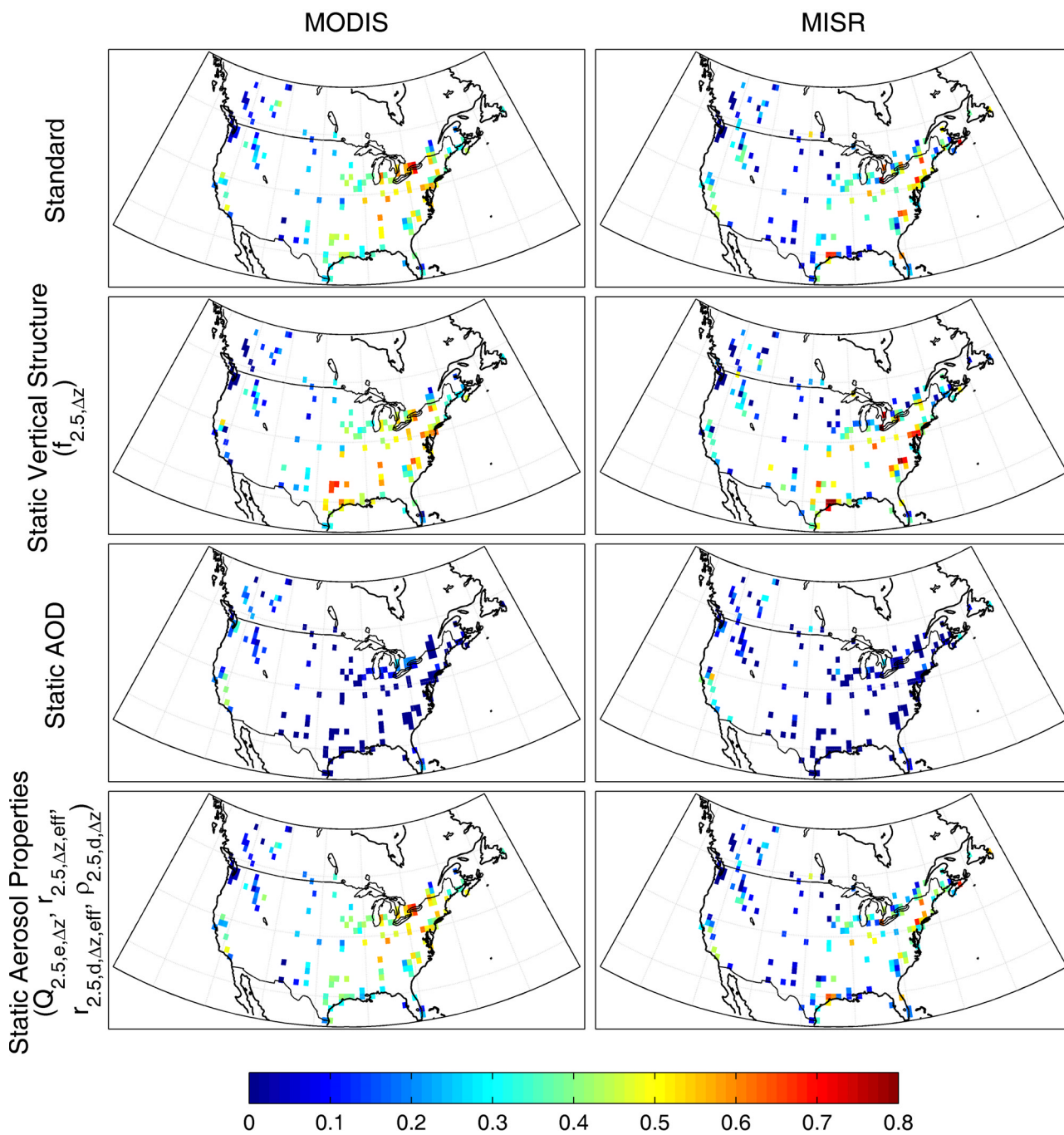


**Figure 4.** Temporal correlation between daily remote and surface measurements of PM<sub>2.5</sub> between January 2001 and October 2002 for a standard case and three sensitivity studies in which parameters in equation (4) are temporally invariant. Correlations have minimum AOD measurements on either 40% of days for MODIS or 8% of days for MISR.

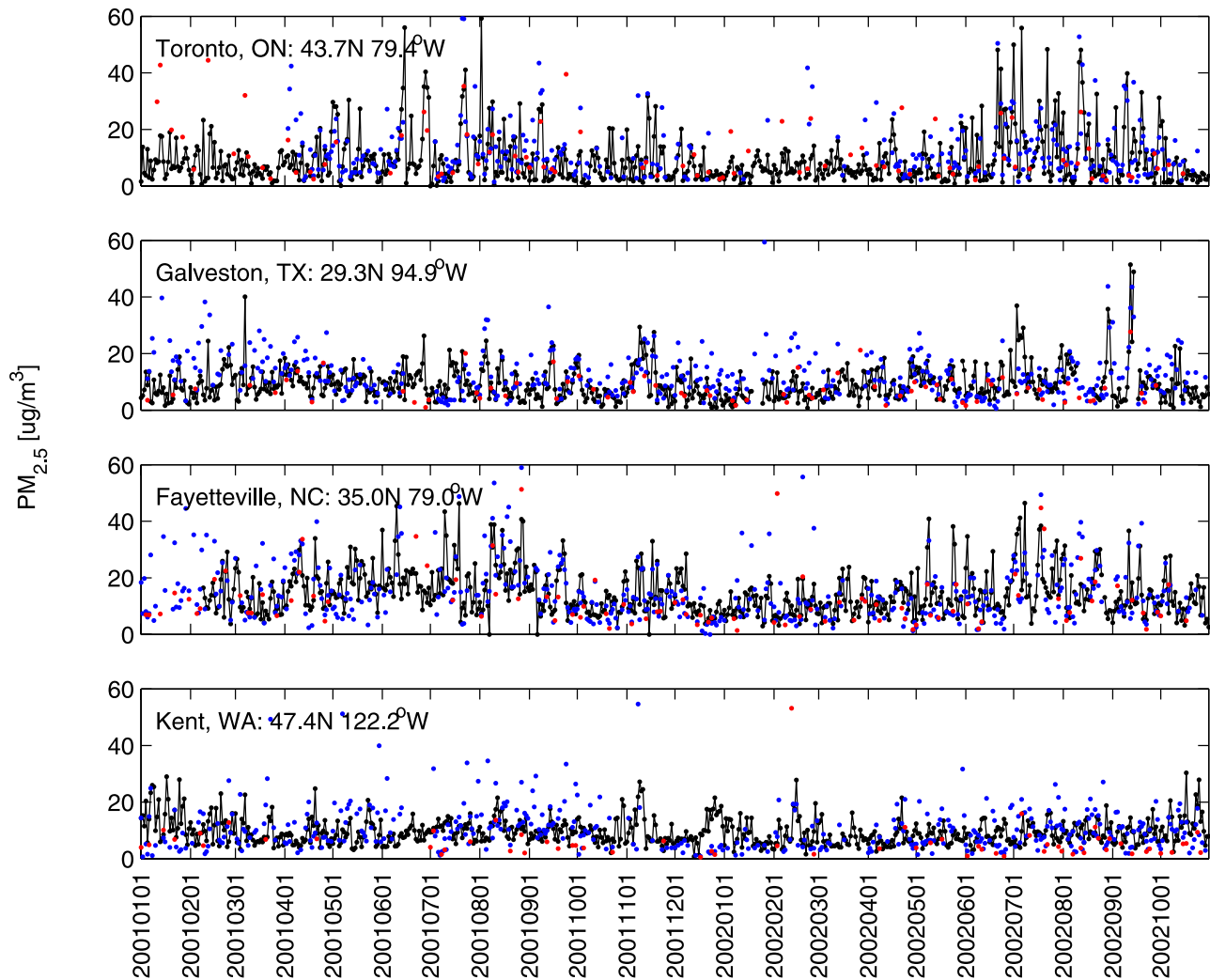


**Figure 5.** Time series plots of mean ground-level PM<sub>2.5</sub> between 1000 and 1200 LT for Toronto, Ontario, Galveston, Texas, Fayetteville, North Carolina, and Kent, Washington. MODIS derived PM<sub>2.5</sub> is plotted in blue, MISR PM<sub>2.5</sub> is plotted in red, and NAPS/AQS PM<sub>2.5</sub> is plotted in black.

surface measurements exist in the east ( $r = 0.5\text{--}0.8$ ) and a poor correlation in the west ( $r < 0.3$ ). Replacing the simulated vertical structure with a constant vertical structure shows that the simulated vertical structure improves slightly the temporal correlation in California, but also slightly decreases agreement in the east. The quality of the temporal correlation is determined largely by the temporal variation in AOD; exclusion of this parameter removes almost all temporal agreement between satellite derived PM<sub>2.5</sub> and surface measurements, with the exception of California for which a moderate correlation ( $r \sim 0.4$ ) remains. The temporal variation of other parameters has an insignificant effect on the relationship between AOD and surface PM<sub>2.5</sub>.

[27] Figure 5 compares time series of surface PM<sub>2.5</sub> at four sites and the satellite retrieval. Overall correlations at these sites for MODIS and MISR, respectively, are: Toronto, Ontario:  $r = 0.67$ ,  $r = 0.35$ ; Galveston, Texas:  $r = 0.34$ ,  $r = 0.48$ ; Fayetteville, North Carolina:  $r = 0.53$ ,  $r = 0.48$ ; and Kent, Washington:  $r = 0.09$ ,  $r = -0.11$ . MODIS PM<sub>2.5</sub> measurements in Kent show a distinct loss in accuracy during June–October, remaining much closer to NAPS/

AQS PM<sub>2.5</sub> during other times of the year. As a result, Kent's overall correlation is quite low, typical of the northwestern United States as shown in Figure 4. MODIS cannot capture AOD measurements over Toronto during winter because of the presence of snow, coinciding with a time in which MISR PM<sub>2.5</sub> shows a loss of consistency with surface measurements. The Toronto region exhibits one of the strongest correlations between remote PM<sub>2.5</sub> and NAPS/AQS PM<sub>2.5</sub>. Wang and Christopher [2003] found similarly high correlations in Jefferson County, Alabama.

## 5. Global PM<sub>2.5</sub>

[28] We tentatively extend our approach to produce a global field of surface PM<sub>2.5</sub>. Figure 6 shows average AOD retrieved from both the MODIS and MISR for January 2001 to October 2002. The largest enhancements are from mineral dust over and downwind of deserts [Kaufman *et al.*, 2005]. Substantial AOD are measured by both MODIS and MISR over eastern China and northern India, associated with industrial pollution and dust storms

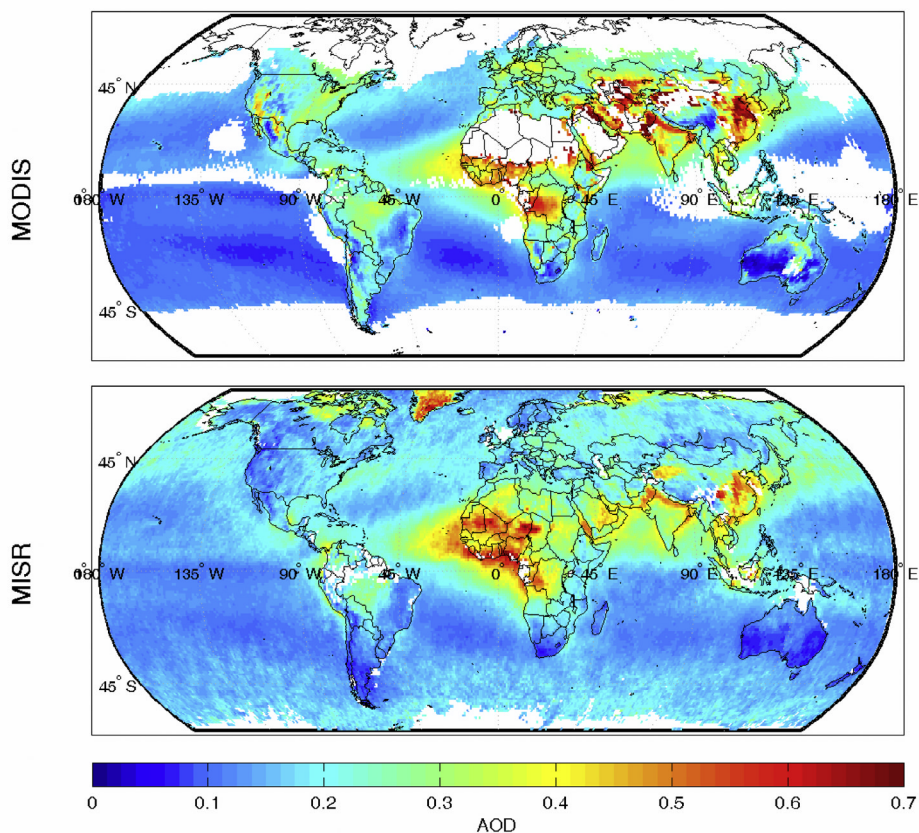


**Figure 6.** Average AOD for January 2001 to October 2002 determined from MODIS and MISR. White space denotes regions with AOD measurements on fewer than either 40% of days for MODIS or 8% of days for MISR.

[Chu *et al.*, 2005; Kahn *et al.*, 2004]. MISR AOD is higher than MODIS AOD over ocean by approximately 0.03 [Abdou *et al.*, 2005]. Over land MODIS AOD is generally higher than MISR AOD by 0.05–0.15, although differences over the Middle East and southwestern United States can reach 0.35. Nonlinearity in the relationship between the infrared and visible surface reflectivity for different land types contributes to the MODIS AOD bias over deserts [Kaufman *et al.*, 2002; Abdou *et al.*, 2005].

[29] Figure 7 shows annual average global remote-sensed PM<sub>2.5</sub>. Pronounced differences with Figure 6 are driven by large spatial variation in equation (4). The spatial patterns are similar for MODIS and MISR ( $r = 0.90$ ), with enhancements over major industrial regions and central Africa. MODIS PM<sub>2.5</sub> tend to be within 2–5  $\mu\text{g}/\text{m}^3$  of MISR PM<sub>2.5</sub>, except MODIS exceeds MISR by 10–15  $\mu\text{g}/\text{m}^3$  for parts of China, eastern United States and northern Europe. Both MODIS and MISR show the largest PM<sub>2.5</sub> concentrations in Northern India and China, with values in excess of 40  $\mu\text{g}/\text{m}^3$ . The meteorology, topography and aerosol sources in the Gangetic valley of India favor the development of high PM<sub>2.5</sub> concentrations [Di Girolamo *et al.*, 2004], contributing to the regional values of 40–50  $\mu\text{g}/\text{m}^3$ . Ground-based measurements of PM<sub>2.5</sub> in China indicate annual average concentrations of 50–100  $\mu\text{g}/\text{m}^3$ , because of dense population coupled with the use of coal and heavy traffic [Zhang *et al.*, 2004; Oanh *et al.*, 2006]. Low PM<sub>2.5</sub> concentrations are

found over and downwind of the Sahara, despite high AOD. The weak relation between AOD and surface PM<sub>2.5</sub> in this region are driven by intense vertical mixing and a large coarse aerosol fraction. Southern Africa displays enhanced surface aerosol concentrations where large seasonal biomass burning occurs [Formenti *et al.*, 2003].

[30] The World Health Organization released in 2005 an air quality guideline for annual mean PM<sub>2.5</sub> concentrations of 10  $\mu\text{g}/\text{m}^3$ . We estimate from the remote-sensed PM<sub>2.5</sub> that at least 70% of the world's population lives in regions that do not meet this standard.

## 6. Conclusions

[31] We estimated the ground-level concentration of fine particulate mass (PM<sub>2.5</sub>) for January 2001 to October 2002 using space-based measurements from the Moderate Resolution Imaging Spectroradiometer (MODIS) and the Multi-angle Imaging Spectroradiometer (MISR) satellite instruments, and additional information from a global chemical transport model (GEOS-CHEM). Remote-sensed PM<sub>2.5</sub> was compared with surface measurements throughout Canada from the National Air Pollution Surveillance (NAPS) network and throughout the United States from the Air Quality System (AQS).

[32] The spatial variation in annual mean PM<sub>2.5</sub> exhibited significant agreement with surface measurements when



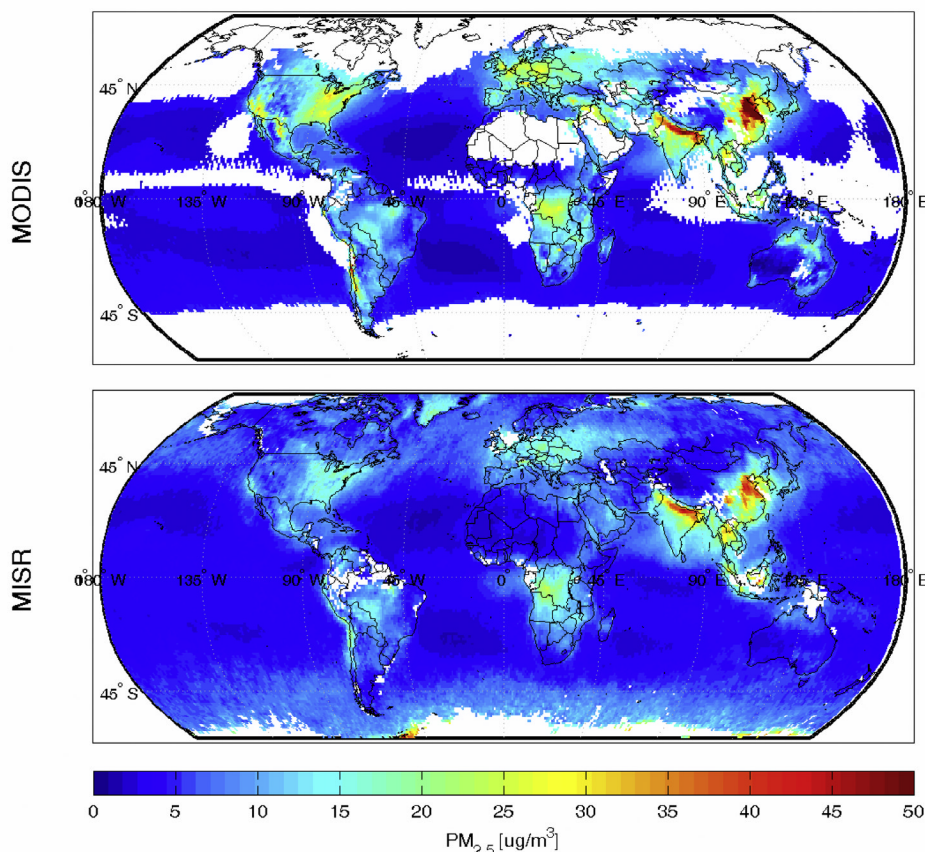


**Figure 7.** Average of daily surface PM<sub>2.5</sub> concentrations for January 2001 to October 2002 determined from MODIS and MISR measurements of AOD. White space denotes regions with AOD measurements on fewer than either 40% of days for MODIS or 8% of days for MISR.

derived from MODIS ( $r = 0.69$ , slope = 0.82), and MISR ( $r = 0.58$ , slope = 0.57). The daily variation in remote-sensed PM<sub>2.5</sub> was more consistent with surface measurements in eastern North America ( $r = 0.5–0.8$ ) than in the western North America ( $r = 0–0.35$ ) for both MODIS and MISR. We validated the method by deriving PM<sub>2.5</sub> from AERONET AOD and found a consistent agreement ( $r = 0.71$ , slope = 0.69) with the surface measurement of PM<sub>2.5</sub>. Removing California from the comparison increases the correlation and slope to 0.61 and 0.68 for MISR and 0.80 and 0.89 for AERONET, with little effect on the comparison with MODIS.

[33] We developed an expression to isolate the most important factors affecting the relationship between ground-level PM<sub>2.5</sub> and AOD. The relative vertical profile of aerosol extinction is the dominant parameter in determining the spatial variation between AOD and PM<sub>2.5</sub> over North America. Simulation of this information in GEOS-CHEM improves the spatial correlation of remote and surface PM<sub>2.5</sub> from 0.36–0.37 to 0.58–0.69. In contrast, daily variation in AOD played the major role in accurately representing daily variation in remote-sensed PM<sub>2.5</sub>. Daily variation in parameters such as the relative vertical profile of aerosol extinction or the effective radius was insignificant.

[34] We developed a global map of mean PM<sub>2.5</sub> using MODIS and MISR measurements of AOD and GEOS-CHEM to relate AOD and PM<sub>2.5</sub>. Large spatial variation in the relationship between AOD and PM<sub>2.5</sub> contributes to

substantial differences in PM<sub>2.5</sub> versus AOD. Northern India and East Asia exhibit pronounced PM<sub>2.5</sub> enhancements of 40–50  $\mu\text{g}/\text{m}^3$ . Annual mean concentrations of 15–25  $\mu\text{g}/\text{m}^3$  are found over eastern North America, Europe, and the biomass burning region of central Africa. Despite large AOD over and downwind of the Sahara, low PM<sub>2.5</sub> concentrations (<5  $\mu\text{g}/\text{m}^3$ ) result from strong vertical mixing and a large coarse aerosol fraction.

[35] Satellite measurements of AOD have the potential to provide a unique synopsis of global surface PM<sub>2.5</sub> concentrations when coupled with additional information from a chemical transport model on the relationship between AOD and PM<sub>2.5</sub>. Development of this capability will depend on the quality of aerosol remote sensing and model simulation of aerosol parameters. Further work should examine the role of internal versus external mixtures in the relationship between AOD and PM<sub>2.5</sub>. Additional constraints on the vertical profile of aerosol extinction from the CALIOP lidar [Winker *et al.*, 2004] should further improve satellite remote sensing of PM<sub>2.5</sub>.

[36] **Acknowledgments.** We are grateful to the MODIS, MISR, NAPS, AQS and AERONET teams for making available data used here. Ray Hoff, Ray Rogers, Ian Folkins, and Glen Lesins provided helpful comments that improved the manuscript. Work at Harvard was funded by the EPA-STAR program. This work was supported by the Natural Sciences and Engineering Research Council of Canada.

## References

- Abdou, W. A., D. J. Diner, J. V. Martonchik, C. J. Bruegge, R. A. Kahn, B. J. Gaitley, and K. A. Crean (2005), Comparison of coincident Multiangle Imaging Spectroradiometer and Moderate Resolution Imaging Spectroradiometer aerosol optical depths over land and ocean scenes containing Aerosol Robotic Network sites, *J. Geophys. Res.*, *110*, D10S07, doi:10.1029/2004JD004693.
- Al-Saadi, J., et al. (2005), Improving national air quality forecasts with satellite aerosol observations, *Bull. Am. Meteorol. Soc.*, *86*(9), 1249–1264.
- Atkinson, R. W., et al. (2001), Acute effects of particulate air pollution on respiratory admissions, *Am. J. Respir. Crit. Care Med.*, *164*, 1860–1866.
- Blanchard, C. L., and S. Tanenbaum (2003), Trends in ambient NO<sub>x</sub> and particulate nitrate concentrations in California, 1980–2000, final report, *CRC Proj., A-43c*, Coord. Res. Council, Inc., Alpharetta, Ga.
- Chin, M., D. L. Savoie, B. J. Huebert, A. R. Bandy, D. C. Thornton, T. S. Bates, P. K. Quinn, E. S. Saltzman, and W. J. De Bruyn (2000), Atmospheric sulfur cycle simulated in the global model GOCART: Comparison with field observations and regional budgets, *J. Geophys. Res.*, *105*(D20), 24,689–24,712.
- Chu, D. A., Y. J. Kaufman, G. Zibordi, J. D. Chern, J. Mao, C. Li, and B. N. Holben (2003), Global monitoring of air pollution over land from the Earth Observing System-Terra Moderate Resolution Imaging Spectroradiometer (MODIS), *J. Geophys. Res.*, *108*(D21), 4661, doi:10.1029/2002JD003179.
- Chu, D. A., et al. (2005), Evaluation of aerosol properties over ocean from Moderate Resolution Imaging Spectroradiometer (MODIS) during ACE-Asia, *J. Geophys. Res.*, *110*, D07308, doi:10.1029/2004JD005208.
- Chung, S. H., and J. H. Seinfeld (2002), Global distribution and climate forcing of carbonaceous aerosols, *J. Geophys. Res.*, *107*(D19), 4407, doi:10.1029/2001JD001397.
- Cooke, W. F., C. Liousse, and H. Cachier (1999), Construction of a 1° × 1° fossil fuel emission data set for carbonaceous aerosol and implementation and radiative impact in the ECHAM4 model, *J. Geophys. Res.*, *104*(D18), 22,137–22,162.
- Di Girolamo, L., T. C. Bond, D. Bramer, D. J. Diner, F. Fettinger, R. A. Kahn, J. V. Martonchik, M. V. Ramana, V. Ramanathan, and P. J. Rasch (2004), Analysis of Multi-angle Imaging Spectroradiometer (MISR) aerosol optical depths over greater India during winter 2001–2004, *Geophys. Res. Lett.*, *31*, L23115, doi:10.1029/2004GL021273.
- Engel-Cox, J. A., C. H. Holloman, B. W. Coutant, and R. M. Hoff (2004a), Qualitative and quantitative evaluation of MODIS satellite sensor data for regional and urban scale air quality, *Atmos. Environ.*, *38*, 2495–2509.
- Engel-Cox, J. A., R. M. Hoff, and A. D. J. Haymet (2004b), Recommendations on the use of satellite remote-sensing data for urban air quality, *J. Air Waste Manage. Assoc.*, *54*, 1360–1371.
- Engel-Cox, J. A., G. S. Young, and R. M. Hoff (2005), Application of satellite remote-sensing data for source analysis of fine particulate matter transport events, *J. Air Waste Manage. Assoc.*, *55*, 1389–1397.
- Formenti, P., W. Elbert, W. Maenhaut, J. Haywood, S. Osborne, and M. O. Andreae (2003), Inorganic and carbonaceous aerosols during the Southern African Regional Science Initiative (SAFARI 2000) experiment: Chemical characteristics, physical properties, and emission data for smoke from African biomass burning, *J. Geophys. Res.*, *108*(D13), 8488, doi:10.1029/2002JD002408.
- Hirsch, R. M., and E. J. Gilroy (1984), Methods of fitting a straight line to data: Examples in water resources, *Water Resour. Bull.*, *20*(5), 705–711.
- Holben, B. N., et al. (1998), AERONET—A federated instrument network and data archive for aerosol characterization, *Remote Sens. Environ.*, *66*(1), 1–16.
- Holben, B. N., et al. (2001), An emerging ground-based aerosol climatology: Aerosol optical depth from AERONET, *J. Geophys. Res.*, *106*(D11), 12,067–12,097.
- Hu, R.-M., R. V. Martin, and T. D. Fairlie (2006), Global retrieval of columnar aerosol single scattering albedo from space-based observations, *J. Geophys. Res.*, doi:10.1029/2005JD006832, in press.
- Jacob, D. J. (2000), Heterogeneous chemistry and tropospheric ozone, *Atmos. Environ.*, *34*, 2131–2159.
- Kahn, R. (2004), Environmental snapshots from ACE-Asia, *J. Geophys. Res.*, *109*, D19S14, doi:10.1029/2003JD004339.
- Kahn, R. A., B. J. Gaitley, J. V. Martonchik, D. J. Diner, and K. A. Crean (2005), Multiangle Imaging Spectroradiometer (MISR) global aerosol optical depth validation based on 2 years of coincident Aerosol Robotic Network (AERONET) observations, *J. Geophys. Res.*, *110*, D10S04, doi:10.1029/2004JD004706.
- Kaufman, Y. J., D. Tanré, L. A. Remer, E. F. Vermote, D. A. Chu, and B. N. Holben (1997), Operational remote sensing of tropospheric aerosol over the land from EOS moderate resolution imaging spectroradiometer, *J. Geophys. Res.*, *102*, 17,051–17,061.
- Kaufman, Y. J., N. Gobron, B. Pinty, J.-L. Widlowski, and M. M. Verstraete (2002), Relationship between surface reflectance in the visible and mid-IR used in MODIS aerosol algorithm - theory, *Geophys. Res. Lett.*, *29*(23), 2116, doi:10.1029/2001GL014492.
- Kaufman, Y. J., I. Koren, L. A. Remer, D. Tanr, P. Ginoux, and S. Fan (2005), Dust transport and deposition observed from the Terra-Moderate Resolution Imaging Spectroradiometer (MODIS) spacecraft over the Atlantic Ocean, *J. Geophys. Res.*, *110*, D10S12, doi:10.1029/2003JD004436.
- Liu, H., D. J. Jacob, I. Bey, and R. M. Yantosca (2001), Constraints from <sup>210</sup>Pb and <sup>7</sup>Be on wet deposition and transport in a global three-dimensional chemical tracer model driven by assimilated meteorological fields, *J. Geophys. Res.*, *106*(D11), 12,109–12,128.
- Liu, Y., R. J. Park, D. J. Jacob, Q. Li, V. Kilaru, and J. A. Samat (2004a), Mapping annual mean ground-level PM<sub>2.5</sub> concentrations using Multiangle Imaging Spectroradiometer aerosol optical thickness over the contiguous United States, *J. Geophys. Res.*, *109*, D22206, doi:10.1029/2004JD005025.
- Liu, Y., J. A. Samat, B. A. Coull, P. Koutrakis, and D. J. Jacob (2004b), Validation of Multiangle Imaging Spectroradiometer (MISR) aerosol optical thickness measurements using Aerosol Robotic Network (AERONET) observations over the contiguous United States, *J. Geophys. Res.*, *109*, D06205, doi:10.1029/2003JD003981.
- Liu, Y., J. A. Samat, V. Kilaru, D. J. Jacob, and P. Koutrakis (2005), Estimating ground-level PM<sub>2.5</sub> in the eastern United States using satellite remote sensing, *Environ. Sci. Technol.*, *39*, 3269–3278.
- Malm, W. C., B. A. Schichtel, M. L. Pitchford, L. L. Ashbaugh, and R. A. Eldred (2004), Spatial and monthly trends in speciated fine particle concentration in the United States, *J. Geophys. Res.*, *109*, D03306, doi:10.1029/2003JD003739.
- Martin, R. V., D. J. Jacob, R. M. Yantosca, M. Chin, and P. Ginoux (2003), Global and regional decreases in tropospheric oxidants from photochemical effects of aerosols, *J. Geophys. Res.*, *108*(D3), 4097, doi:10.1029/2002JD002622.
- Martonchik, J. V., D. J. Diner, K. A. Crean, and M. A. Bull (2002), Regional aerosol retrieval results from MISR, *IEEE Trans. Geosci. Remote Sens.*, *40*(7), 1520–1531.
- Martonchik, J. V., D. J. Diner, R. Kahn, B. Gaitley, and B. N. Holben (2004), Comparison of MISR and AERONET aerosol optical depths over desert sites, *Geophys. Res. Lett.*, *31*, L16102, doi:10.1029/2004GL019807.
- Oanh, N. T. K., et al. (2006), Particulate air pollution in six Asian cities: Spatial and temporal distributions, and associated sources, *Atmos. Environ.*, *40*(18), 3367–3380.
- Park, R. J., D. J. Jacob, M. Chin, and R. V. Martin (2003), Sources of carbonaceous aerosols over the United States and implications for natural visibility, *J. Geophys. Res.*, *108*(D12), 4355, doi:10.1029/2002JD003190.
- Park, R. J., D. J. Jacob, B. D. Field, and R. M. Yantosca (2004), Natural and transboundary pollution influences on sulphate-nitrate-ammonium aerosols in the United States: Implications for policy, *J. Geophys. Res.*, *109*, D15204, doi:10.1029/2003JD004473.
- Park, R. J., D. J. Jacob, N. Kumar, and R. M. Yantosca (2006), Regional visibility statistics in the United States: Natural and transboundary pollution influences and implications for the Regional Haze Rule, *Atmos. Environ.*, *40*(28), 5405–5423.
- Pope, C. A., III, R. T. Burnett, M. J. Thun, E. E. Calle, D. Krewski, K. Ito, and G. D. Thurston (2002), Lung cancer, cardiopulmonary mortality, and long-term exposure to fine particulate air pollution, *J. Am. Med. Assoc.*, *287*(9), 1132–1141.
- Remer, L. A., et al. (2005), The MODIS aerosol algorithm, products and validation, *J. Atmos. Sci.*, *62*, 947–973.
- Wang, J., and S. A. Christopher (2003), Intercomparison between satellite-derived aerosol optical thickness and PM<sub>2.5</sub> mass: Implications for air quality studies, *Geophys. Res. Lett.*, *30*(21), 2095, doi:10.1029/2003GL018174.
- Wang, Y. X., M. B. McElroy, D. J. Jacob, and R. M. Yantosca (2004), A nested grid formation for chemical transport over Asia: Applications to CO, *J. Geophys. Res.*, *109*, D22307, doi:10.1029/2004JD005237.
- Winker, D. M., W. H. Hunt, and C. A. Hostetler (2004), Status and performance of the CALIOP lidar, *Proc. SPIE Int. Soc. Opt. Eng.*, *5575*, 8–15.
- Zhang, Y., X. Zhu, S. Slanina, M. Shao, L. Zeng, M. Hu, M. Bergin, and L. Salmon (2004), Aerosol pollution in some Chinese cities (IUPAC technical report), *Pure Appl. Chem.*, *76*(6), 1227–1239.

R. V. Martin and A. van Donkelaar, Department of Physics and Atmospheric Science, Dalhousie University, Halifax, NS, Canada B3H 3J5. (adonkela@dal.ca)

R. J. Park, Division of Engineering and Applied Sciences, Harvard University, Cambridge, MA 02138, USA.